

Supporting Information

© Wiley-VCH 2012

69451 Weinheim, Germany

Selective Visual Detection of TNT at the Sub-Zeptomole Level**

*Ammu Mathew, P. R. Sajanlal, and Thalappil Pradeep**

anie_201203810_sm_miscellaneous_information.pdf

Table of contents

Number	Description	Page no.
	Instrumentation	2
SI-1	Characterization of various MFs and their hybrid forms	3-4
SI-2	Characterization of Ag ₁₅ @BSA	5
SI-3	Dark field microscopic study of various MFs functionalized with Ag ₁₅	6-7
SI-4	Effect of TNT on the luminescence of Ag ₁₅ in solution phase and at single particle level	8
SI-5	Effect of varying TNT concentration and other compounds on the absorption spectra of Ag ₁₅ in solution	9
SI-6	Variation of intensity of emission of Ag ₁₅ @BSA in solution with the addition of equal amounts of various MFs	10
SI-7	Raman spectra of solid TNT and effect of addition of other compounds to luminescent Au/Ag@Ag ₁₅ MF	11
SI-8	Effect of luminescence of the cluster with various metal ions in solution phase and at on single particles	12

Instrumentation

Scanning electron microscopic (SEM) images and energy dispersive analysis of X-ray (EDAX) images were obtained using a FEI QUANTA-200 SEM. For the SEM and EDAX measurements, samples were spotted on a carbon tape and dried in ambient condition. Luminescence measurements were carried out on a Jobin Yvon NanoLog instrument. The bandpass for excitation and emission was set as 5 nm. Raman measurements were done with a WiTec GmbH, Alpha-SNOM CRM 200 confocal Raman microscope having a 633 nm laser as the excitation source. This excitation source (instead of 532 nm) was used to suppress the cluster emission. For Raman studies, the material was carefully transferred onto a cover glass and dried in ambience. Then the MF-coated glass plates were mounted on the sample stage of the confocal Raman microscope. A supernotch filter placed in the path of the signal effectively cuts off the excitation radiation. The signal was then dispersed using a 600 grooves/mm grating, and the dispersed light was collected by a Peltier cooled charge coupled device (CCD). Matrix assisted laser desorption ionization mass spectrometric (MALDI MS) studies were conducted using a Voyager DE PRO Biospectrometry Workstation (Applied Biosystems) matrix assisted laser desorption ionization time-of-flight mass spectrometer (MALDI TOF MS). UV-vis spectra were recorded using Perkin Elmer Lambda 25 UV-vis spectrometer. Spectra were typically measured in the range of 200-1100 nm.

Dark-field microscopy/spectroscopy of the gold mesoflowers

Dark-field imaging of the gold MFs was done using an Olympus BX-51 microscope and 100 W quartz halogen light source on a CytoViva microscope set-up. Here, a broadband white light was shown on the particles from an oblique angle via a dark field condenser. The scattered/emitted light from the particle was collected by a 100x oil immersion objective and imaged by a true-color charge-coupled device (CCD) camera or by a spectrophotometer. Each spectrum shown (in Figure S3H, for example) is collected from a single pixel and is approximately 64 nm in size. Spectral analysis was performed with hyperspectral image analysis software. For fluorescence imaging, a mercury lamp light source is used. Light after passing through specific excitation (bandpass) filter falls on the sample. The emitted light was passed through a 460-500 nm band pass filter and fluorescence (if any) emitted by the particle was imaged or the spectrum was collected with a spectrometer.

Supporting information 1

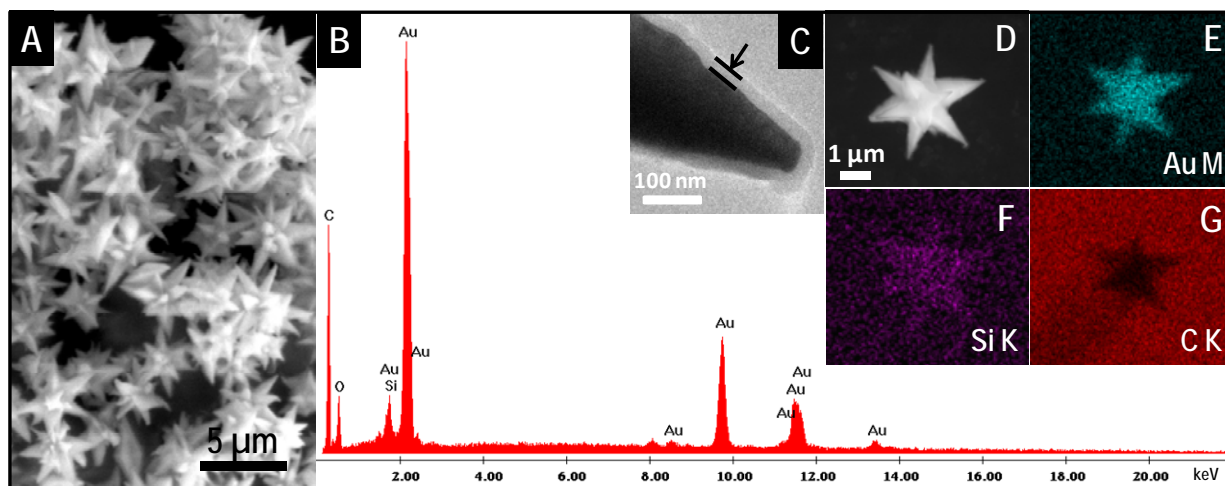


Figure S1a. (A) Large area SEM image and (B) EDAX spectrum of Au@SiO₂ MFs, (C) a magnified TEM image of the tip of the MF showing the uniform silica coating on its surface (shown with an arrow) and (D-G) SEM and corresponding EDAX images of a single MF showing the presence of Au M α , and Si K α on the MF. Carbon is from the substrate used for measurement.

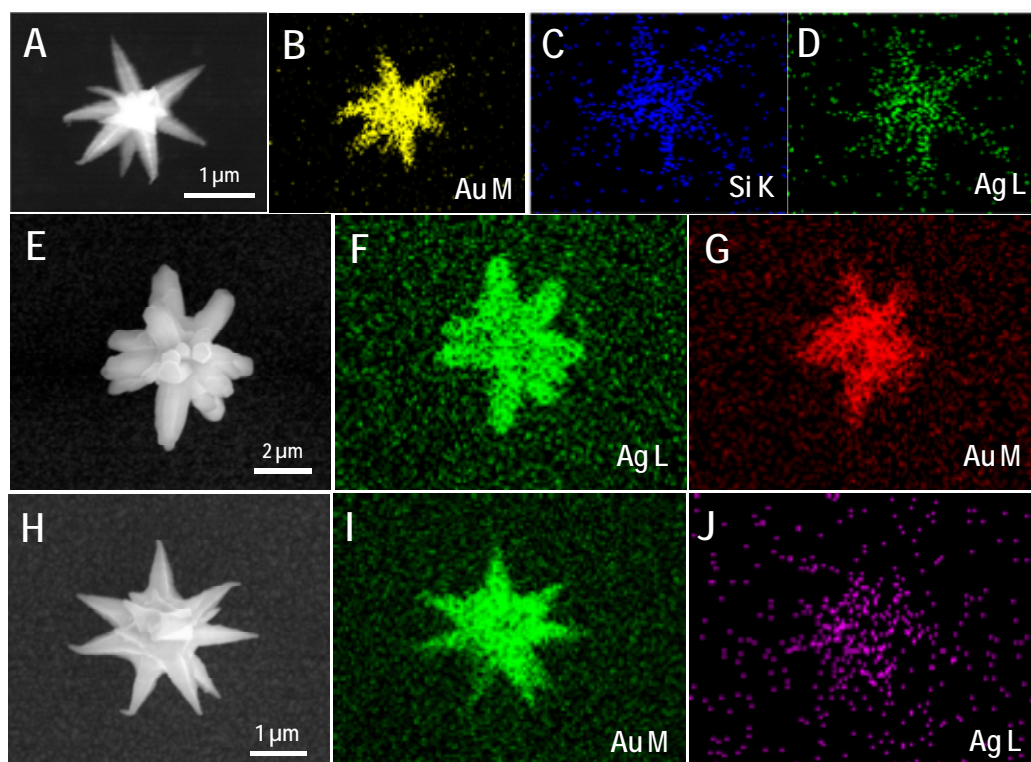


Figure S1b. SEM and EDAX characterization of the various cluster-loaded hybrid MFs used in this study, (A-D) Au@SiO₂@Ag₁₅ MF, (E-G) Au/Ag@Ag₁₅ MF and (H-J) Au@Ag₁₅MF. Coating of cluster on the MF surface is evident from the EDAX map of Ag L on the MFs.

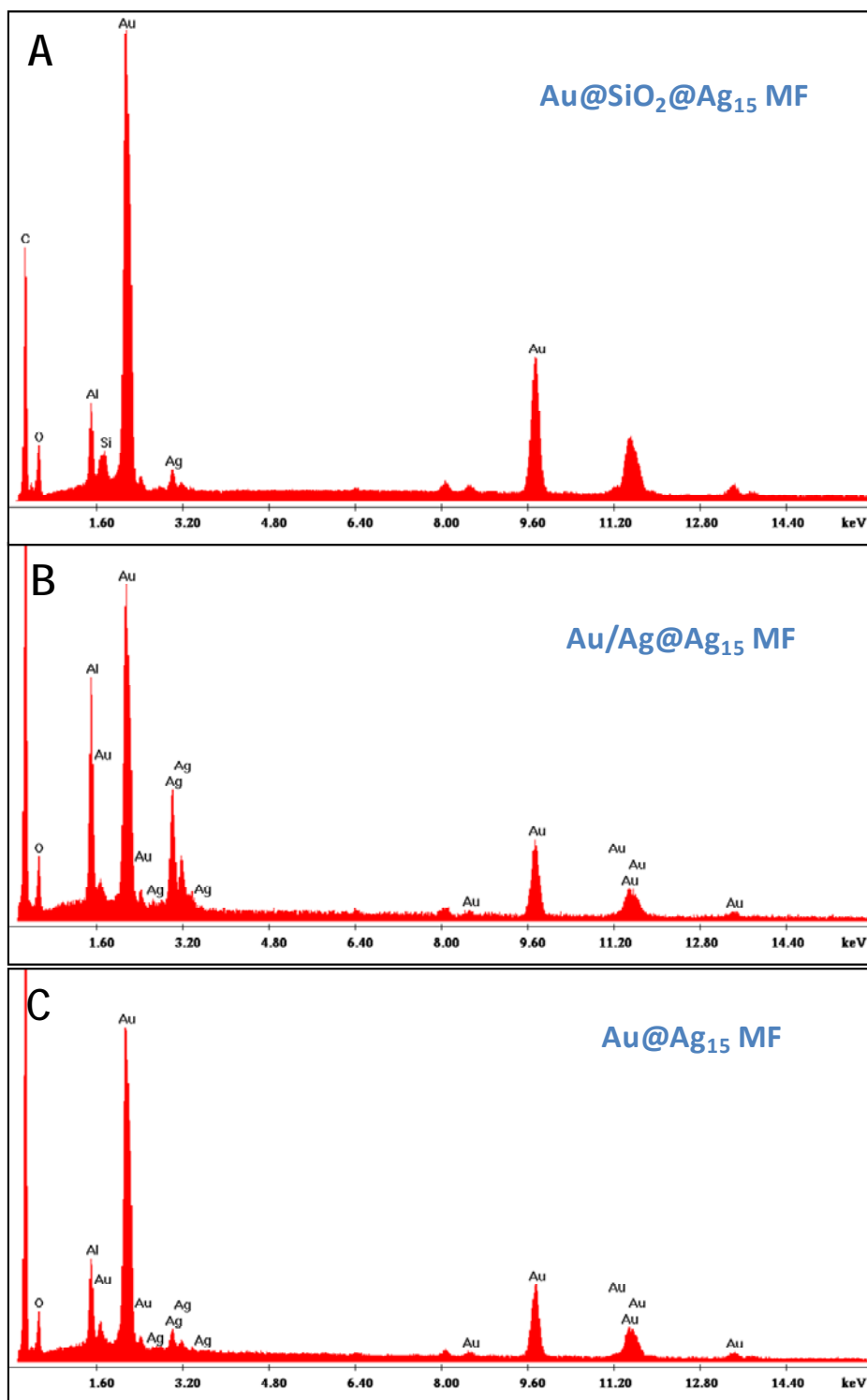


Figure S1c. EDAX spectra of the various cluster-loaded MFs (A) Au@SiO₂@Ag₁₅ MF, (B) Au/Ag@Ag₁₅ MF and (C) Au@Ag₁₅ MF. Carbon and aluminium are from the substrate used for the measurement.

Supporting information 2

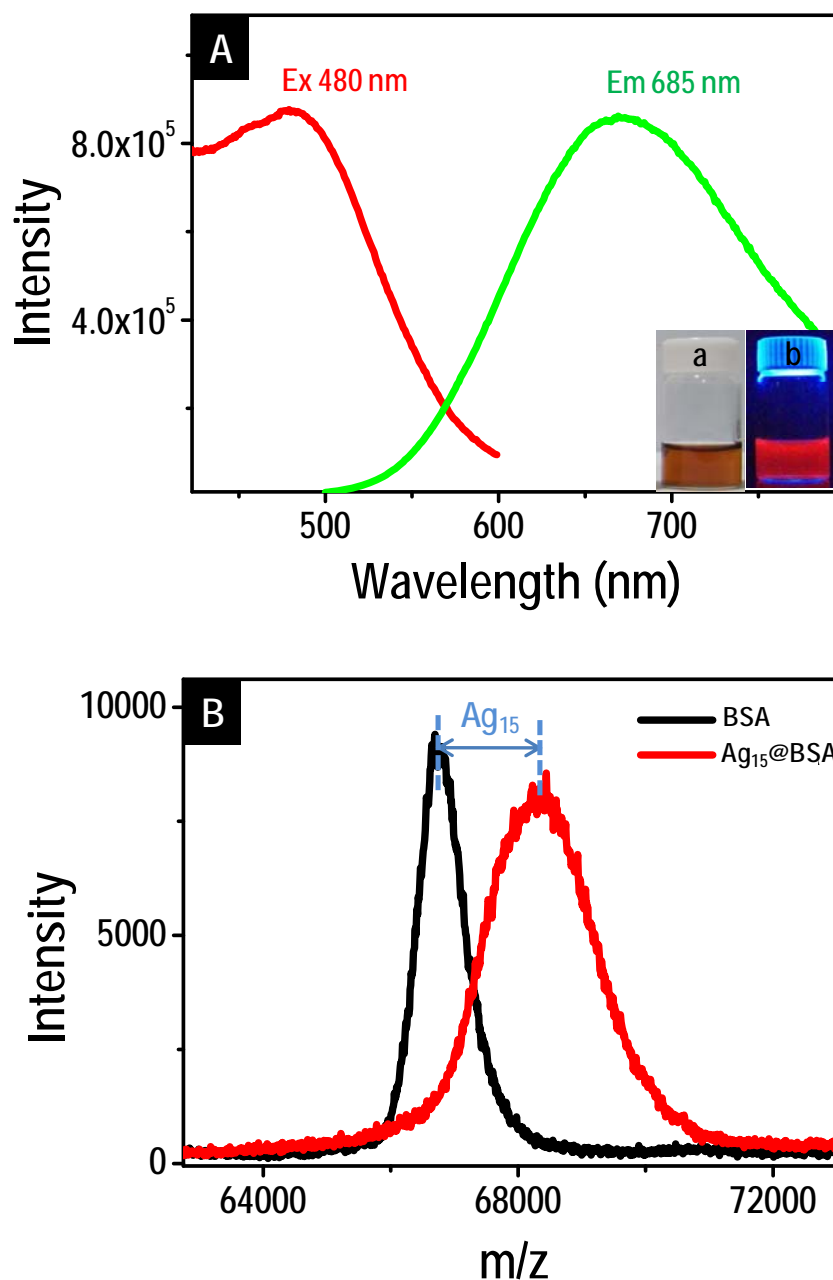


Figure S2. (A) Luminescence profile of cluster solution (Ag₁₅@BSA). Inset shows photographs of the cluster solution under visible light (a) and UV light (b). (B) MALDI MS of BSA (black trace) and cluster collected in linear positive ion mode using sinapic acid as the matrix (red trace). A mass difference corresponding to 15 atoms of silver was observed in case of cluster compared to that of bare protein and the cluster was assigned as Ag₁₅@BSA. The cluster was stable and had a bright red luminescence (as shown in the figure) at room temperature with a quantum yield of 10.7%.

Supporting information 3

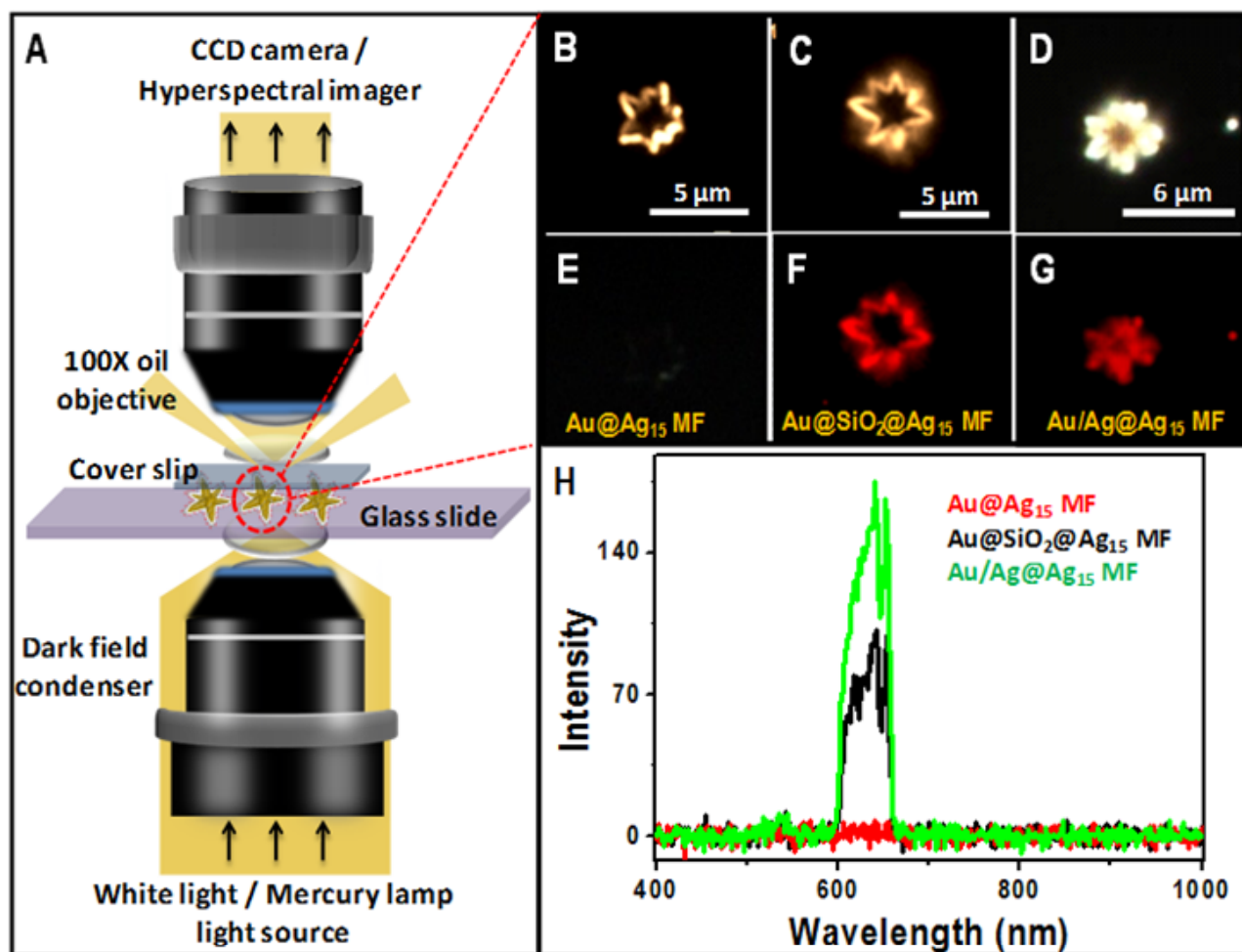


Figure S3a. (A) Schematic of the hyperspectral microscopic set-up used for collecting the images of the MFs. Optical and fluorescence images of (B, E) Au@Ag₁₅ MF, (C, F) Au@SiO₂@Ag₁₅ MF and (D, G) Au/Ag@Ag₁₅ MF obtained using a dark field fluorescence microscope, respectively. Corresponding spectra collected from the surface of the MF in each case is also shown in (H). The emitted light passes through a triple pass filter which cuts off the excitation light. SEM and EDAX characterization of the three types of MFs shown above is given in Figure S1b and c. The luminescence of Ag₁₅ is completely quenched on bare Au MF.

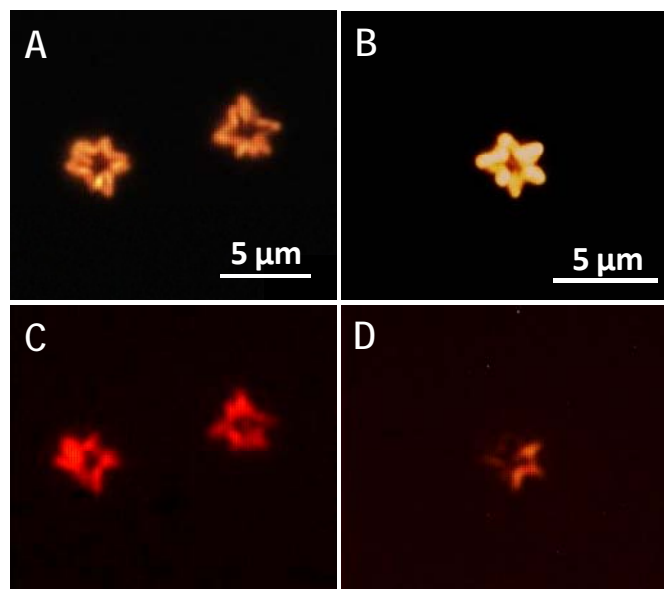


Figure S3b. (A, C) White light and fluorescence images of the as-prepared Au@SiO₂@Ag₁₅ MFs. (B, D) Images collected from the same glass slide after 1 month in ambient conditions. The enhanced stability of the otherwise easily oxidised silver clusters (under laboratory conditions) could be attributed to them getting embedded in the silica layer. Note that different particles are imaged in A and B.

Supporting information 4

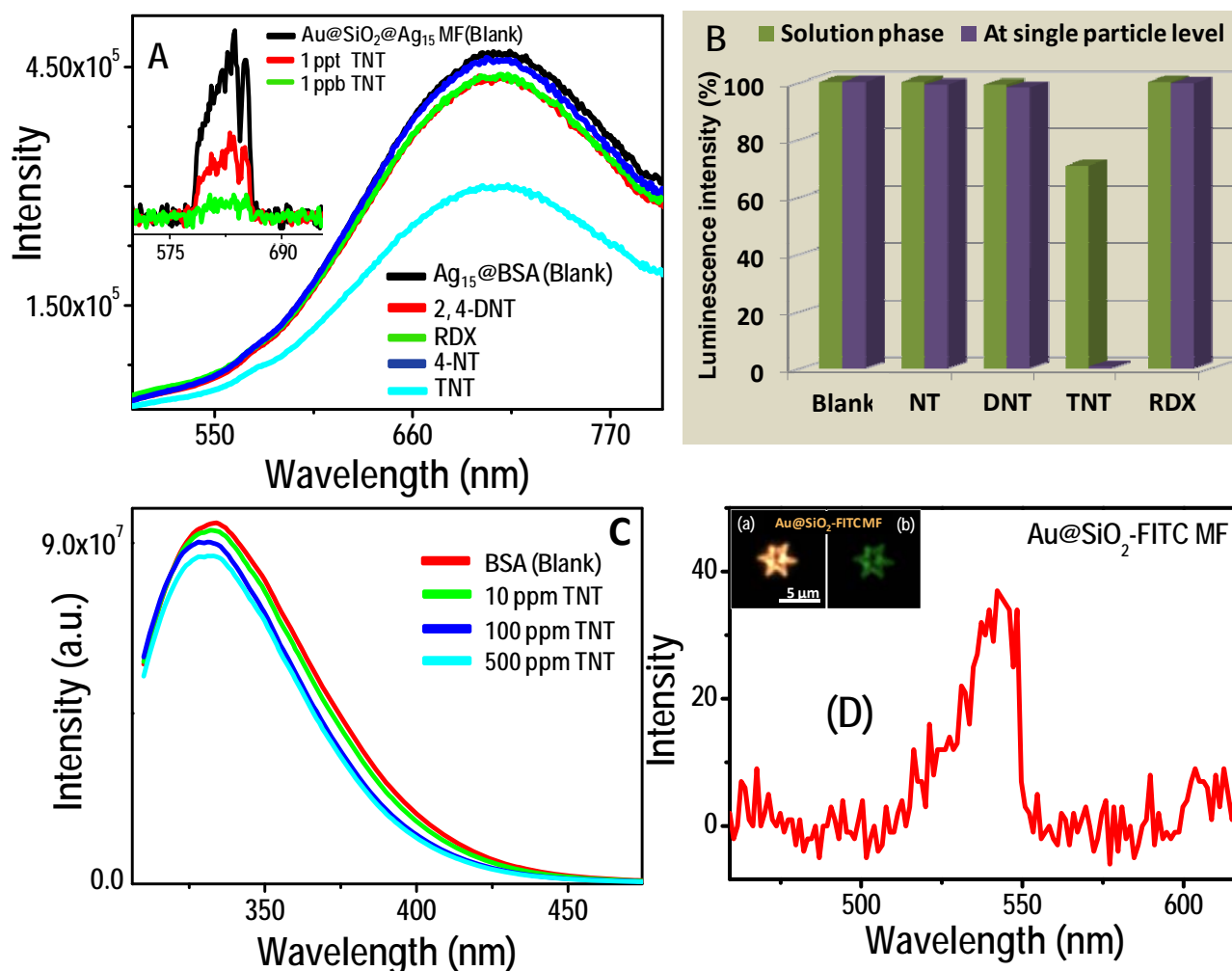


Figure S4. (A) Luminescence spectra collected after adding 100 ppm of various compounds into the Ag₁₅ cluster solution. Inset shows the luminescence spectra collected from Au@SiO₂@Ag₁₅ MF upon exposure to various concentrations of TNT. (B) Bar diagram shows the comparison of luminescence quenching phenomena at solution phase and single particle level upon exposure to various analytes (all at 100 ppm). (C) Emission spectra illustrating the effect of bare protein, BSA, with 0.1 mL of various concentrations of TNT solution indicated in the figure. Absence of any significant quenching of protein luminescence in presence of TNT indicates the importance of the cluster utilised. (D) The luminescence spectrum collected from Au@SiO₂-FITC MF. The emission is from the FITC molecules attached on Au@SiO₂ MF. Inset shows the optical (a) and fluorescence images (b) of Au@SiO₂-FITC MF.

Supporting information 5

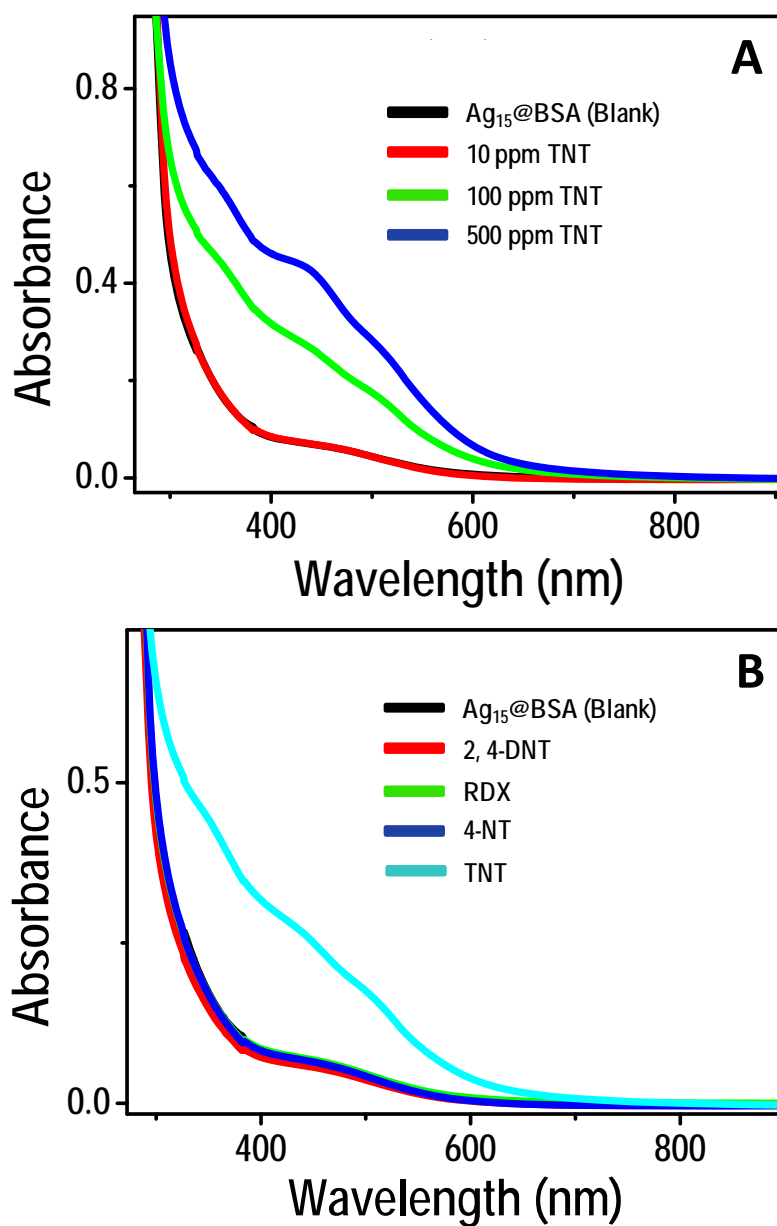


Figure S5. UV-vis absorption spectra showing the effect of cluster solution with (A) various concentrations of TNT solution and (B) various nitro compounds and RDX. Spectral features appearing at 340, 450 and 525 nm in case of higher concentration of TNT is due to the formation of the Meisenheimer complex and the resultant solution turned dark red in color. No such changes were observed for 2, 4-DNT, RDX and 4-NT.

Supporting information 6

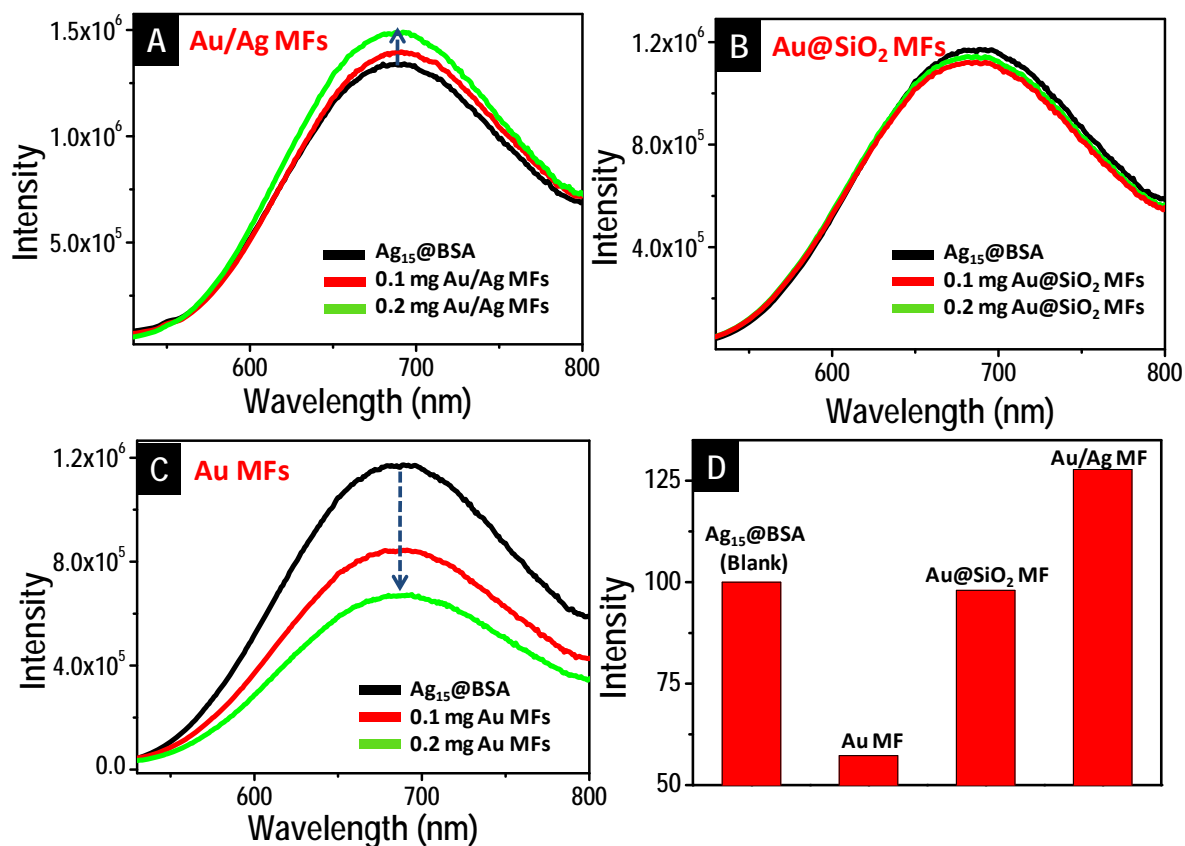


Figure S6. (A-C) Variation of emission spectra of the $\text{Ag}_{15}@BSA$ solution upon addition of equal amounts of various MFs. (D) Bar diagram showing the relative effect of luminescence intensity of the cluster solution with 0.2 mg of various MFs. While luminescence quenching was observed in the case of Au MFs, retention of the luminescence intensity of cluster solution was demonstrated by Au@ SiO_2 MFs due to the silica layer on the MF surface which acts as a spacer between the Au surface and the cluster. Bimetallic Au/Ag MFs showed an enhancement of luminescence intensity of the cluster solution due to metal enhanced luminescence.

Supporting information 7

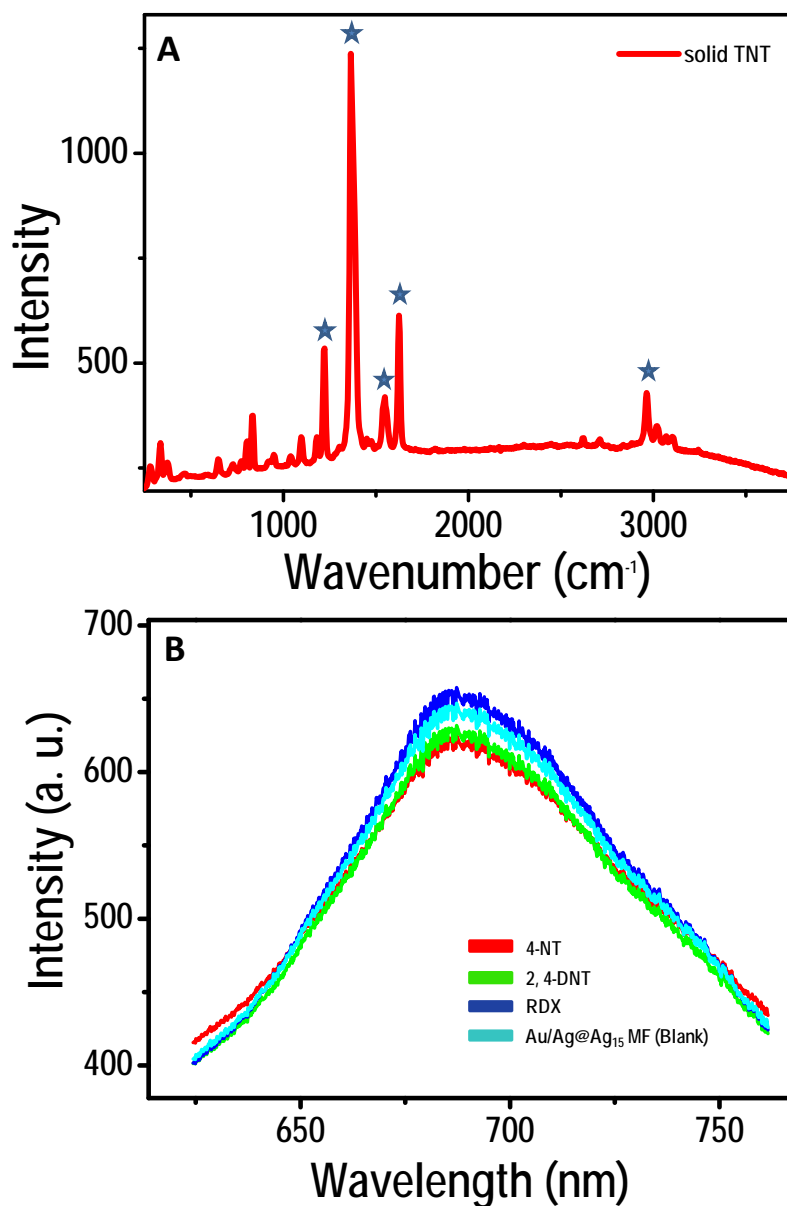


Figure S7. (A) Raman spectra of solid TNT. Prominent features of TNT due to C₆H₂-C vibration [1218 cm⁻¹], -NO₂ symmetric stretching vibration [1366 cm⁻¹ (strong)], NO₂ asymmetric stretching vibration [1545 cm⁻¹ (weak)], C=C aromatic stretching vibration [1629 cm⁻¹] and C-H stretching and CH₂ asymmetric stretching [2965 cm⁻¹] are marked on the spectra. (B) Raman spectra showing the effect of addition of 4-nitrotoluene (4-NT), 2,4-dinitrotoluene (2,4-DNT) and RDX to the luminescent Au/Ag@Ag₁₅ MFs. A broad background due to the luminescence from the cluster on the MF surface was only observed.

Supporting information 8

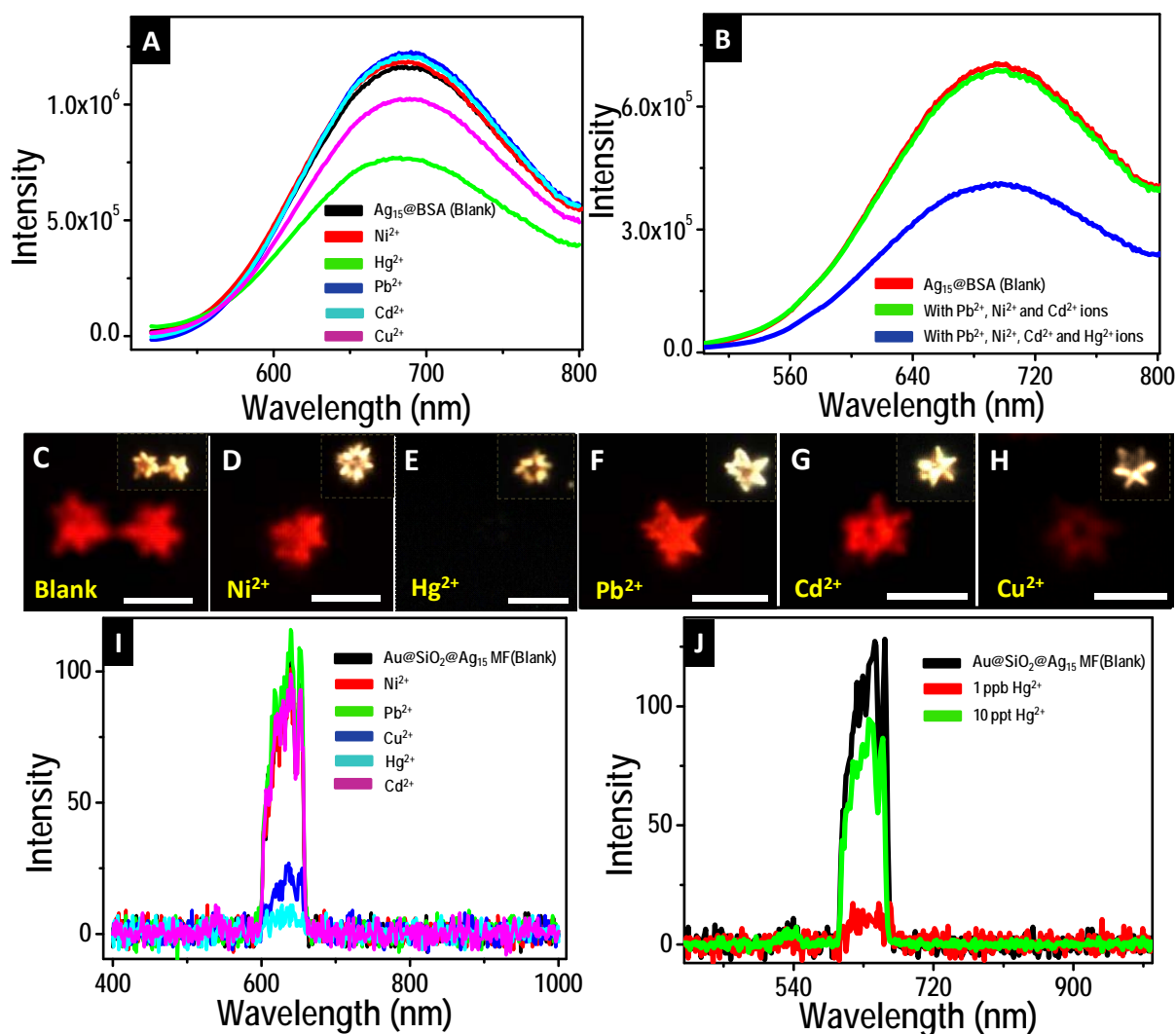


Figure S8. Effect of cluster luminescence in solution with 100 ppm concentration of each metal ion (A) and (B) with a solution containing mixture of metal ions. (C-H) Luminescence images of Au@SiO₂@Ag₁₅ MFs upon exposure to 100 ppm of various metal ions (indicated in each image). Corresponding optical images are shown as the inset of each figure. Scale bars in the images correspond to 5 μm. Corresponding spectra collected from the surface of the MF for 100 ppm concentration of each metal ions is shown in (I). (J) Variation of luminescence intensity of the Au@SiO₂@Ag₁₅ MF after treatment of 1 ppb and 10 ppt concentrations of Hg²⁺ ions. The emitted light passes through a triple pass filter which cuts off the excitation light.